Dislocation Modeling and Comparison with GPS Data to Assess Possible Strain Accumulation in the central Lesser Antilles, Commonwealth of Dominica

Lydia M. Staisch
Senior Integrative Exercise
March 10, 2008

Submitted in partial fulfillment of the requirements for a
Bachelor of Arts degree from Carleton College, Northfield, Minnesota.

Table of Contents

Abstract

Introduction **1**

Geologic Setting **2**
Plate Tectonic *2*
Study Location *7*

Geodetic Data **7**
Data Collection *7*
Data Processing *9*

Subduction Zone Modeling **10**
Dislocation Models *10*
Analyzing model fit with GPS data *18*
Statistical Analysis *20*

Model Results **22**

Discussion **23**
Model and GPS Comparisons *23*
Subduction zone geometry *25*
Comparisons with Previous Studies *26*

Conclusion **31**

Acknowledgements **32**

References **32**

Appendix 1 ..... **36**

Dislocation Modeling and Comparison with GPS Data to Assess Possible Strain Accumulation in the central Lesser Antilles, Commonwealth of Dominica

Lydia M. Staisch
Carleton College
Senior Integrative Exercise
March 10, 2008

Advisors:
Sarah Titus, Carleton College
Glen Mattioli, University of Arkansas, Fayetteville

ABSTRACT

The Lesser Antilles island arc is formed by the ~2 cm/yr convergence of the North and South American plates with the Caribbean Plate. Surface displacements are reported from campaign and continuous GPS observations taken at 28 geodetic benchmarks located in Guadeloupe, Dominica and Aves islands in the central Lesser Antilles. The vertical and horizontal surface displacements for each site were estimated over 2-7 years. These GPS data were used to constrain simple dislocation models of the subduction zone geometry beneath the Caribbean plate. In 88 different models, the angle of the subducting slab, the downdip extent of the locked plate interface, and the percentage of plate interface locking were varied. To find the best parameter combination, a chi-squared, best-fit statistical criterion was applied that yields a subduction interface of 75 kilometer downdip extent, a 10° dip angle, and near 50% locking. The model implies that the subduction zone offshore Dominica is currently in an interseismic state, thus accumulating strain and causing small westward and upward displacement of the Lesser Antilles relative to the stable Caribbean interior.

Keywords: Subduction, GPS, displacements, dislocations, Caribbean Plate, Dominica, Lesser Antilles

INTRODUCTION

The Lesser Antilles island arc, along the eastern edge of the Caribbean plate, is the result of westward subduction of the North and South American plates beneath the Caribbean plate. This active arc represents a significant volcanic and seismic hazard. For example, large earthquakes (M>7.5) have been recorded in the northern and central regions of the arc (Sykes et al., 1965, Stein et al., 1982, Bouysse and Westercamp, 1990) and volcanic eruptions, such as the 1997 Montserrat Soufriere Hills volcano dome collapse, occur along the island arc. The Micotrin volcanic complex of Dominica was the most productive volcanic center of the Lesser Antilles within the past 100 ky, resulting in a submarine pyroclastic fan extending over 250 km from the source (Sigurdsson, 1972). The local and regional tectonic mechanisms are responsible for these hazards.

Surprisingly, the tectonics at this plate boundary are not well understood. The ability to define the Lesser Antilles subduction zone behavior and geometry would aid in characterizing the volcanic and seismic risks. Subduction zone behavior, such as strain accumulation, influences the frequency and magnitide of earthquakes whereas the subduction zone geometry influences the depth, location, and magnitude of earthquakes as well as the location of volcanism. Previous studies using earthquake data have improved the current knowledge of the Lesser Antilles region (Dorel, 1981, Stein et al., 1982, Feuillet et al., 2002). Earthquake hypocenters help constrain the surface of the plate interface and aid in understanding the geometry and seismic nature of the subduction zone. In a study by Feuillet et al. (2002), seismic data from the Lesser Antilles indicate that hypocenter depths increase westward from the subduction trench, ranging from a few kilometers near the surface trace of the plate interface, down to ~220

kilometers beneath the western arc. The plate interface dips at a shallow angle west of the trench and much more steeply under the arc. Additionally, the small radius of curvature of the Lesser Antillean arc implies that the angle between the Caribbean plate and the subducting American plate is small (Wadge and Shepherd, 1984). The deepest seismicity in the region is concentrated just south of Dominica, where the Benioff zone dip is the steepest at about 50-60° (Stein et al., 1982, Bouysse and Westercamp, 1990).

In this study, I investigate the regional subduction geometry in order to assess the strain accumulation along the arc. Subduction zone models based on a dislocation model of an elastic half-space were used (Yamashina, 1976, Savage, 1983). In the models, I varied the subduction zone dip angle, length of the locked downgoing slab extent, and the percentage of interplate coupling. The models predicted vertical and horizontal displacements that were compared to the observed Global Positioning System (GPS) data from Dominica, Guadeloupe and Aves islands in the Lesser Antilles (Dixon, 1991, Davidson et al., 2004, Carr et al., 2006, Graham et al., 2007, Fauria et al., 2007). The comparisons determined a subduction zone geometry that best fits the observed data. These models have important implications for strain accumulation and therefore earthquake hazards in the Lesser Antilles.

GEOLOGIC SETTING

Plate Tectonics

The Lesser Antilles are an ~800 km long volcanic island arc along the eastern edge of the Caribbean plate from Saba in the north to Granada in the south (Macdonald et al., 2000) (Fig. 1). The islands are approximately 125-150 km inboard from the

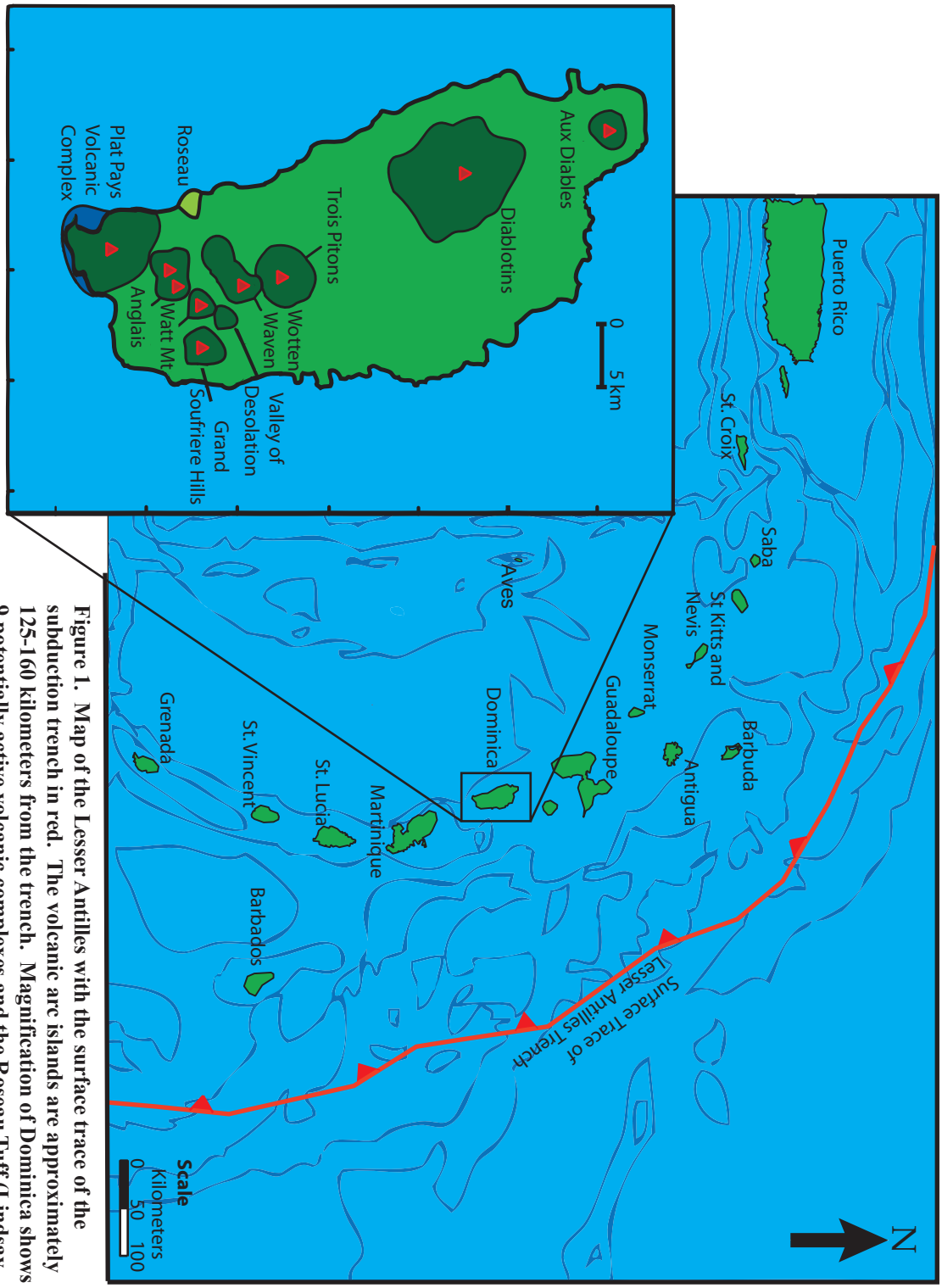

Figure 1. Map of the Lesser Antilles with the surface trace of the subduction trench in red. The volcanic arc islands are approximately 125-160 kilometers from the trench. Magnification of Dominica shows 9 potentially active volcanic complexes and the Roseau Tuff (Lindsay et al., 2005). Figure modified from Bouysse and Westercamp, (1990).

subduction trench where the North and South American plates subduct beneath the Caribbean plate (Fig. 2). The subducting plates consist of very old oceanic lithosphere (~100 my) and the current convergence is orthogonal to the plate boundary at a rate of ~2cm/yr (Stein et al., 1983). The lithosphere age and slip rates are believed to control the geometry of a subduction zone including the dip angle and length of the slab as well as the coupling between the plates (DeMets et al., 2000, DeMets et al., 2007).

Convergence has resulted in an anomalously thick accretionary prism up to 20 km (Speed, 1981). There is no observable topographic trench because the accreted sedimentary cover partially obscures the actual subduction geometry. Also, the North American–South American plate boundary is diffuse in this region (Stein et al., 1982), but may be located near 15°N (Fig. 2) according to seismic and bathymetric data. The South American plate is thought to be dipping beneath Dominica (Bowin, 1976, Mann et al., 1990).

The Barracuda and St. Lucia ridges and the Tiburon rise are allochthonous terranes trending WNW on the North and South American plates (Fig. 3). These topographic features may influence the regional subduction and volcanism when subducted beneath the Caribbean plate (Bouysse and Westercamp, 1990).

The seismicity in the Lesser Antilles is higher in frequency north of 14°N (Tomblin, 1975, Bouysse and Westercamp, 1990) and the deepest seismicity just south of Dominica (Stein et al., 1982). Dorel (1981) suggests that the Benioff zone, the length of the slab interface with the highest seismicity, is steepest (50-60°) in the area where earthquake hypocenters are deepest and that the Benioff zone dip shallows to the north and south. This geometry is consistent with the November 29, 2007 intraplate earthquake

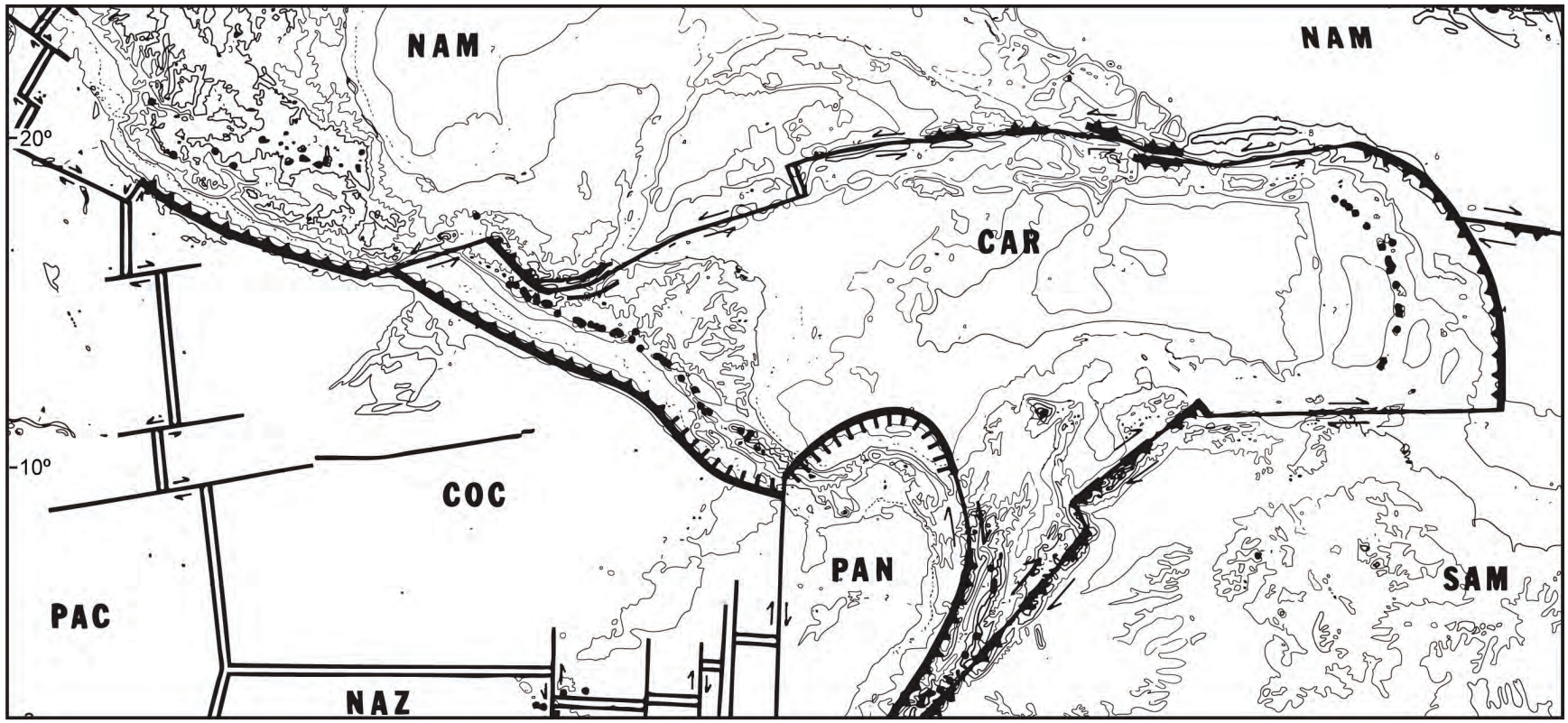

Figure 2. Present plate boundaries. Double lines are extentional and sea-floor spreading sites. Single think lines are locations of strike-slip motion. Single heavy lines indicate surface trace of thrust faulting at sites of compression. All markings of the heavy lines are on the downdip sides; the triangles indication subduction (Bowin, 1976, Mann et al., 1990). Plates are labeled: NAM, North American; SAM, South American; CAR, Caribbean; COC, Cocos; PAC, Pacific; NAZ, Nazca; PAN, Panama block. Contours indicate sea-floor topography. Figure modified from Bowin (1976).

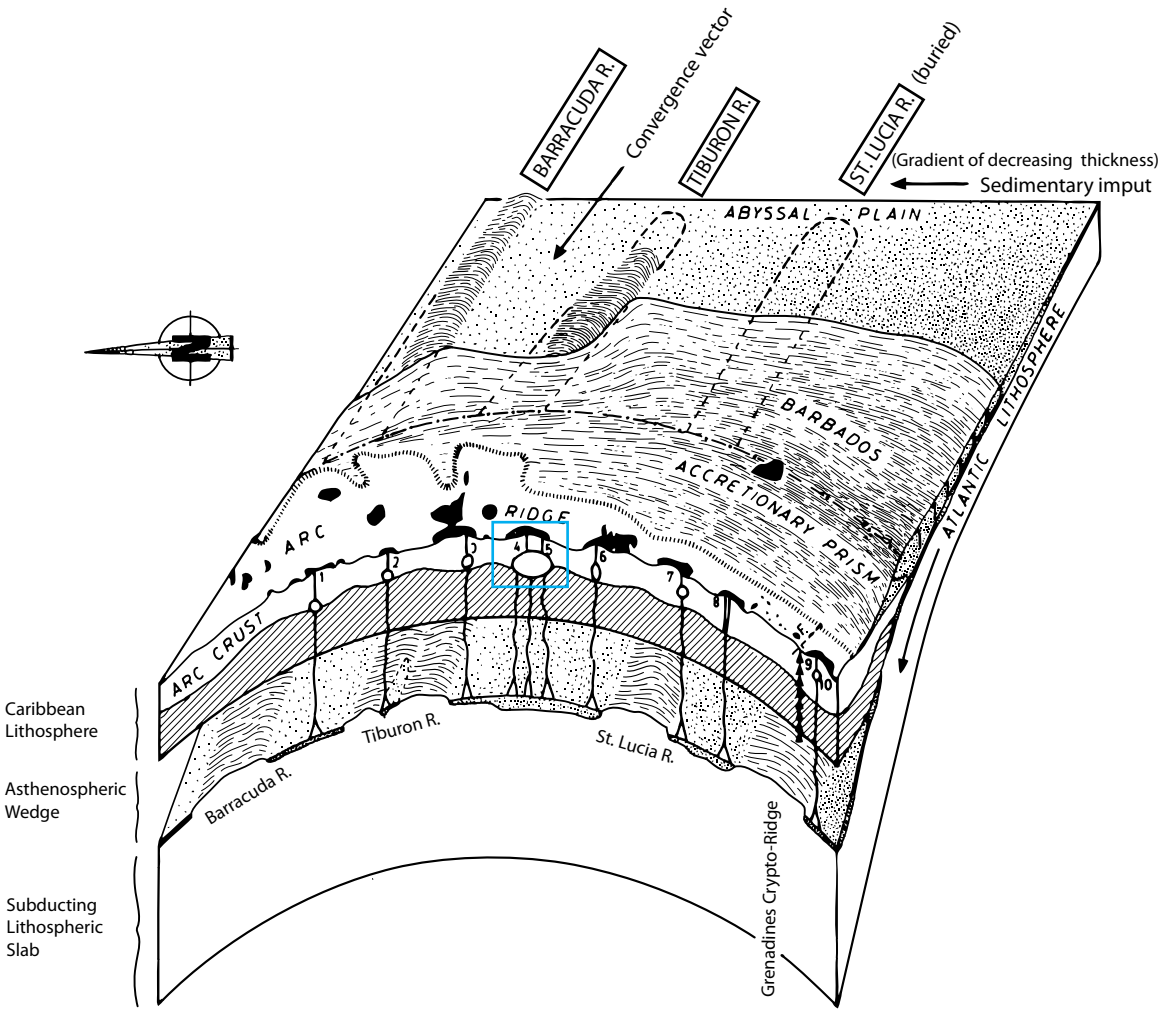

Figure 3. Cross-section showing Barracuda, Tiburon, and St. Lucia allochthonous ridges being subducting beneath the Caribbean lithosphere. These ridges are sources of regional tectonic activity that may influence interplate coupling and deformation of the overlying crust (Bouysse and Westercamp, 1990). Note that Dominica, outlined by the blue box, lies between the Tiburon and St. Lucia ridges, illustrated with a large magma source beneath it.

between Dominica and Martinique that had a hypocenter depth of 147 km (NEIC, 2007). Large regional earthquakes followed by seismically quiet periods characterize the seismicity of the Lesser Antilles (Dorel, 1981).

Study Location

The ~754 km² island of Dominica is located near the center of the Lesser Antillean volcanic arc and consists mainly of hydrothermically altered andesite. The island is highly volcanic in part due to its location at the site of maximum normal convergence between the Caribbean and the North and South American plates (DeMets et al., 2000). Nine volcanic complexes are likely active (Fig. 1; Lindsay et al., 2005). Most volcanoes are clustered near the southern end of the island. In recent years, shallow seismic swarms have occurred in the north and south of the island (SRU, 2000), indicating possible magma movement associated with volcanic or shallow tectonic motions.

GEODETIC DATA

Data collection

In order to measure surficial deformation of Dominica, campaign Global Positioning System (GPS) data was collected from 23 stations that had data from previous campaigns (Davidson et al., 2004, Carr et al., 2006, Graham et al., 2007, Fauria et al., 2007). A variety of GPS receivers (Trimble R7, Ashtech Z-12, and Ashtech μ-Z) and antennae (Ashtech choke ring and Trimble Zephyr) were used to survey the stations. Antennae were set on spike mounts, tetrapods, or tripods (Fig. 4). The distances from

Figure 4. Photograph of GPS antenna and receiver set up at site NVEN. Assembly components are labeled. Steven James for scale.

benchmark to antenna ground planes were measured and later included in site position calculations. Each site recorded data for a minimum of 3 days with at least 8 continuous hours of collection. Site location data points were averaged for every day of collection. Clear sky view is necessary in order to locate at least 3 satellites, and in most areas 6 or more satellites were obtained. All sites acquired and archived data at 30 second epochs with an elevation mark of 5° above the horizon.

Data Processing

GIPSY-OASISII (GPS inferred positioning system – orbit analysis) software, produced by the Jet Propulsion Laboratory, was used to calculate site locations with latitudinal, longitudinal, and vertical ellipsoids (Zumberge et al., 1997). Final precise satellite ephemeris and clock files were also obtained to correct for gravitational field change, ocean tides, pole tides, and ocean loading. Non-fiducial files were used in order to prevent necessary recalculations (as opposed to fiducial files which are tied to a specific reference points which may change) (Heflin et al., 1992). This is the same analysis scheme reported by Jansma and Mattioli (2005). The data collected in 2007 were processed into the International Terrestrial Reference Frame 2005 (ITRF05) and previous survey data from Davidson et al. (2004) and Carr et al. (2006) were reprocessed and updated into the new reference frame. Data points ranging more than two standard deviations away from the average were determined as outliers and removed from the final data set used to calculate the component site velocities.

To derive site velocities, site positions from at least two years are needed. The horizontal and vertical changes for each site data point were averaged over the years of

data collection to attain a surface velocity, measured by the amount of surface displacement in mm/yr (Fig. 5). The error for each site velocity decreases with more years of data collection (Mao et al., 1999).

The ITRF05-fixed displacement vectors reflect several overlapping causes, including eastward motion of the Caribbean plate, deformation of the eastern margin of the Caribbean plate due to plate convergence, regional tectonic influences, and regional volcanism. To better interpret the displacements, site velocities were recalculated relative to a stable Caribbean plate (DeMets et al., 2000). At the time of analysis, the Caribbean pole was only published relative to ITRF00. Orbit and clock parameters from JPL were no longer available after December 2006, thus requiring that all data acquired after that date be analyzed relative to ITRF05. To eliminate motion of the rigid Caribbean plate interior, the Caribbean plate Euler pole was recalculated using the new site locations in Dominica (Fauria et al., 2007). Linear velocities were estimated from the revised Euler pole and subtracted from the raw horizontal velocities (DeMets et al., 2000, Fauria et al., 2007, DeMets et al, 2007). The resulting vectors are interpreted to reflect site position movements caused by the plate convergence and regional tectonic or volcanic influences (Fig. 6 and 7).

SUBDUCTION ZONE MODELING

Dislocation Models

To assess the strain accumulation along the margins of the Caribbean plate, I created dislocation models of strain accumulation and release. Modeling was done using Caltech's DISL software (Larsen, 1992) in an elastic half-space earth model where an

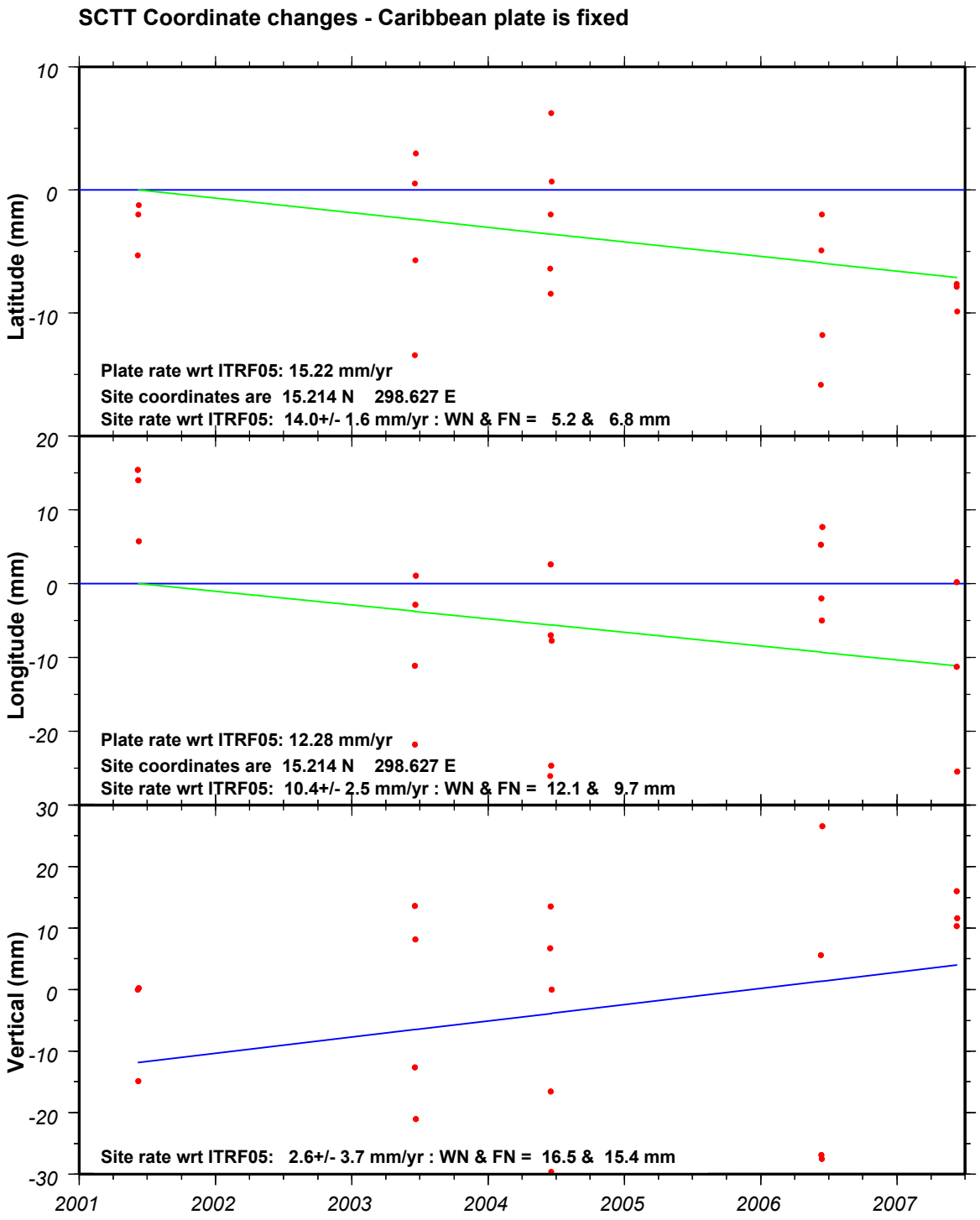

Fig 5. Time series plot for GPS site SCTT. The y-axis is displacement in mm and the x-axis is the year of data collection. Red dots indicate each GPS positive estimate, blue lines indicate rate relative to a fixed Caribbean plate, and green lines indicate best-fit site rate in ITRF05. A steeper slope of the green line means the residual site rate relative to a fixed Caribbean plate is larger. Positive latitude slope depicts movement to the north. Similarly, longitude is positive to the east, as vertical is upwards. Stable Caribbean plate rate derived and subtracted from site rate to acquire site velocity relative to a stable Caribbean plate. Plate rate from DeMets et al., (2007). Formal uncertainties are not shown on each positive estimate for clarity, but are included in the velocity fitting prodedure.

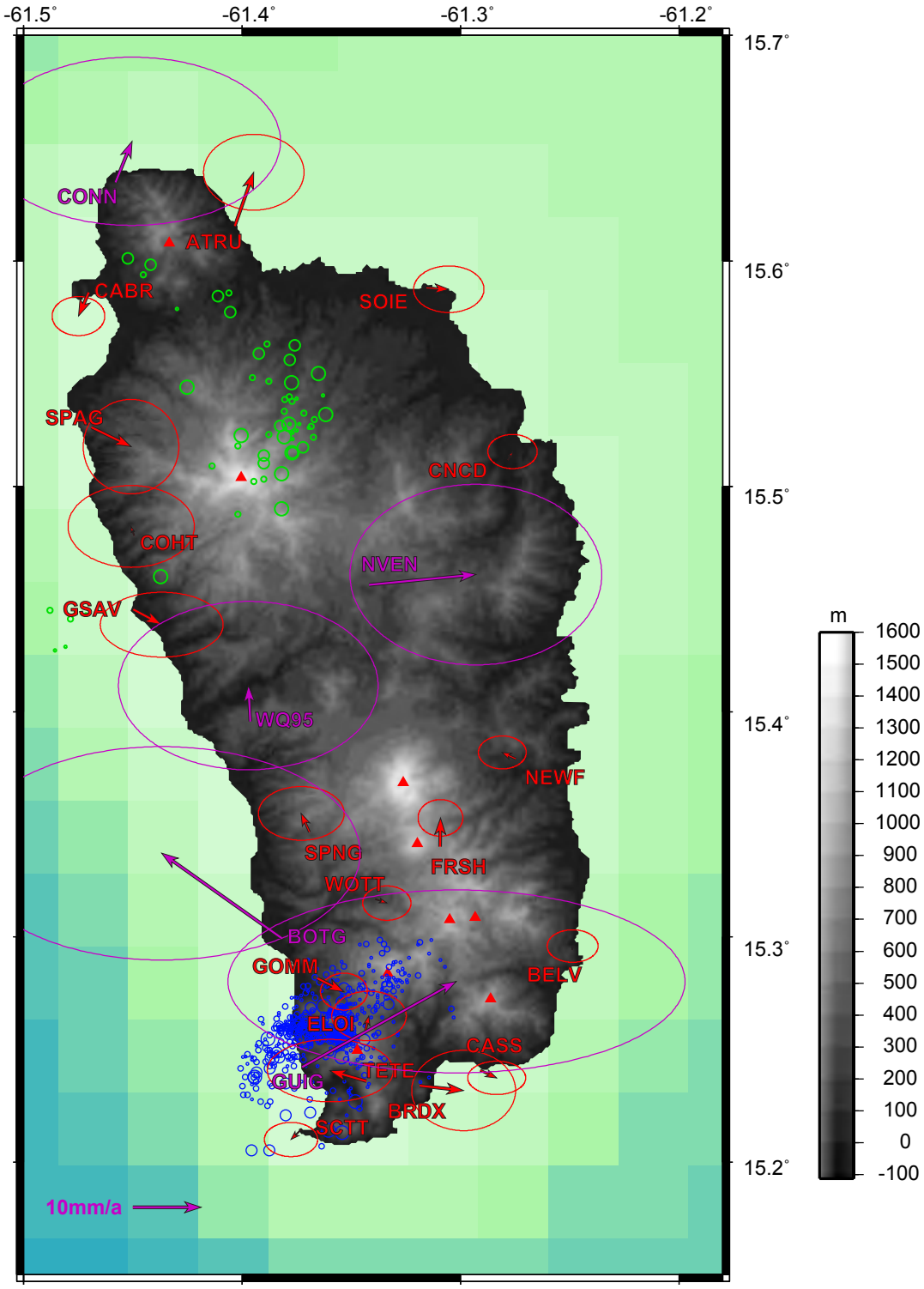

Figure 6. Topographic map of Dominica with observed horizontal GPS vectors and associated error ellipses. Red vectors have at least 3 epochs of data, purple have only two. All data are shown in a Caribbean-fixed reference frame relative to ITRF05. Green and blue circle clusters indicate recent seismic swarm epicenters from 1998 and 2001 (SRU, 2000). Vector scale bar on bottom left, topographic elevation scale on right.

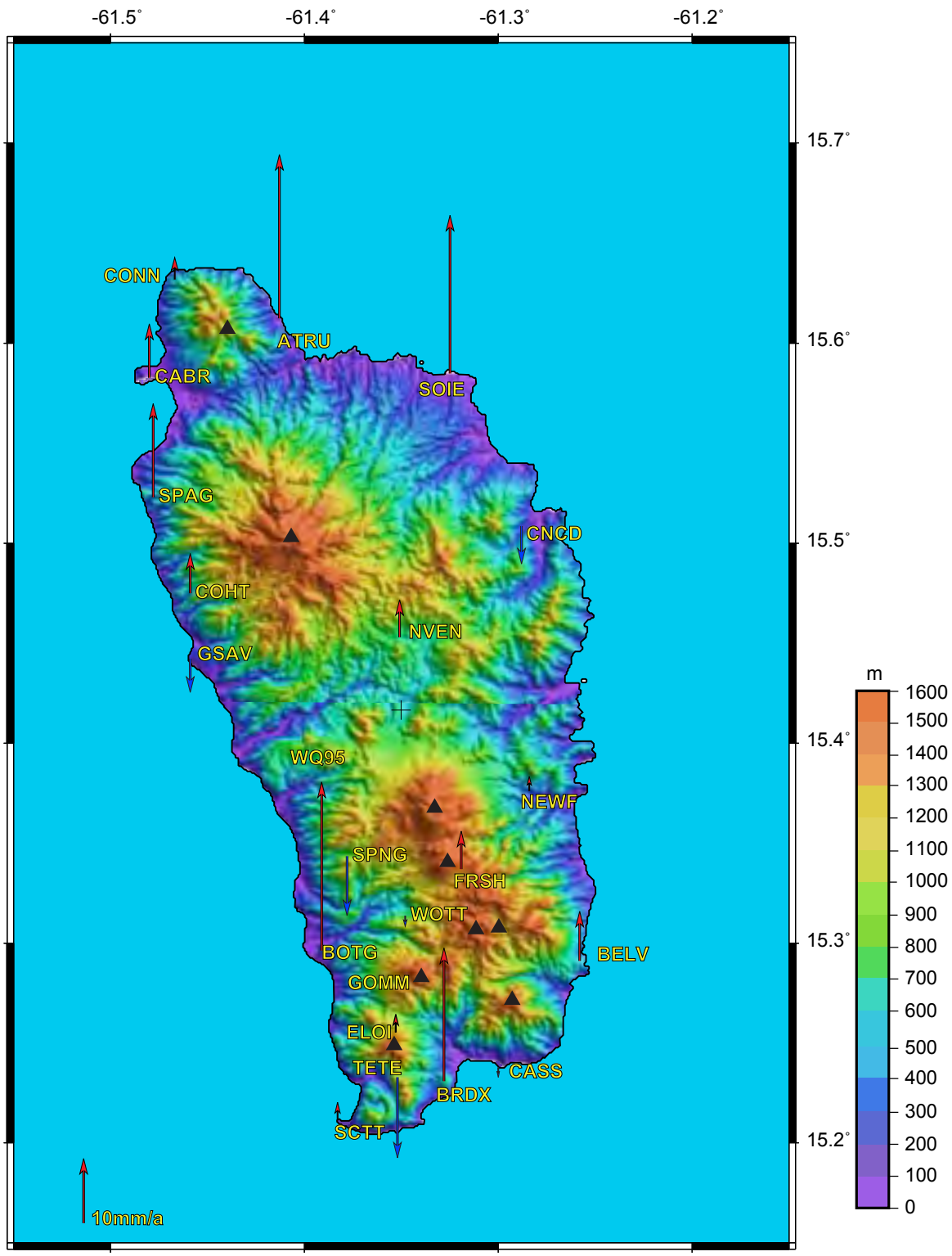

Figure 7. Observed vertical GPS displacement on Dominica. Elevation changes are in height above the ellipsoid (WGS84) and referenced to the Earth's barycenter. Map colors indicate elevation with scale bar on right, red arrows indicate an increase in vertical elevation, and blue arrows indicate a decrease. Vector scale bar on bottom left.

elastic plate floats over a fluid substrate. In a typical dislocation model such as DISL, deformation of the free surface of the overthrust plate consists of an abrupt seismic event, followed by linear recovery during the interseismic period (Fig. 8) and deformation calculations do not account for asthenospheric motions due to lithosphere subduction (Savage, 1983). DISL models were used to calculate the predicted horizontal and vertical displacement along a 2-D transect with the variable subduction zone geometries.

I produced 88 separate finite dislocation models with different subduction zone geometries. A simplified subduction zone geometry was used where the subduction zone orientation was held constant, striking 340° and extending 400 km. The slip rate was also held constant at 2 cm/yr with entirely dip-slip motion based on plate motion rates from DeMets et al. (2000).

The subduction angle, downdip extent of the locked interface, and the percentage of plate interface locking were variable parameters (Fig. 9). Downdip extent refers to the section of a subducting slab extending downward from the trench. Strain accumulates from the coupled converging plates along this length of slab. The percentage of coupling is a measurement of how much frictional force is applied between the converging plates. In a system with 100% locking, slip related to convergence is balanced such that the force is applied between the plates resulting in aseismicity from lack of slip motion along the plate interface and a highly deformed overthrust plate, whereas in a system with 0% locking, there is no friction between the plates and the subduction at the full plate rate is smooth and aseismic. If the plates are partially coupled, there is strain accumulation during an interseismic period resulting in uplift inboard of the trench and shortening of the overthrust lithosphere (Fig 10, A). Strain accumulates until there is a seismic rupture

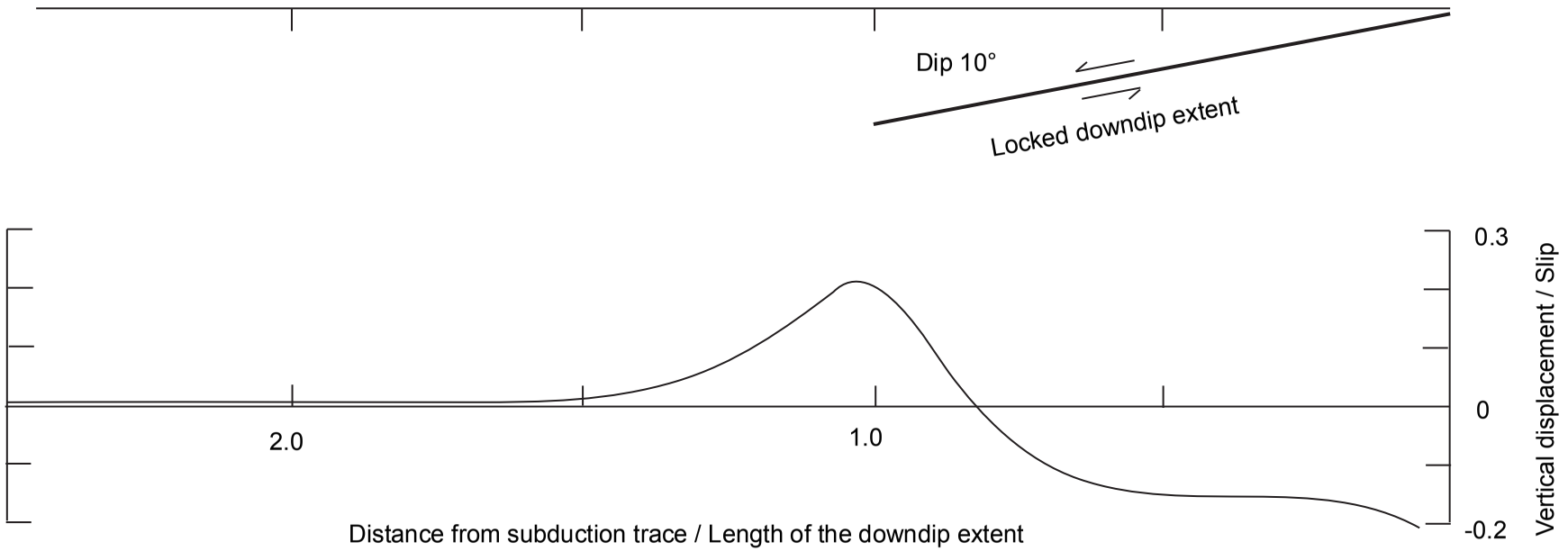

Figure 8. The elastic half-space dislocation model of strain accummulation at a subduction zone. The upper diagram shows a vertical cross section with the downdip locked extent dipping at 10°. The lower figure shows the vertical uplift generated by normal slip along the downdip locked extent that occurs during interseismic intervals of strain accumulation. Figure modified from Savage (1983).

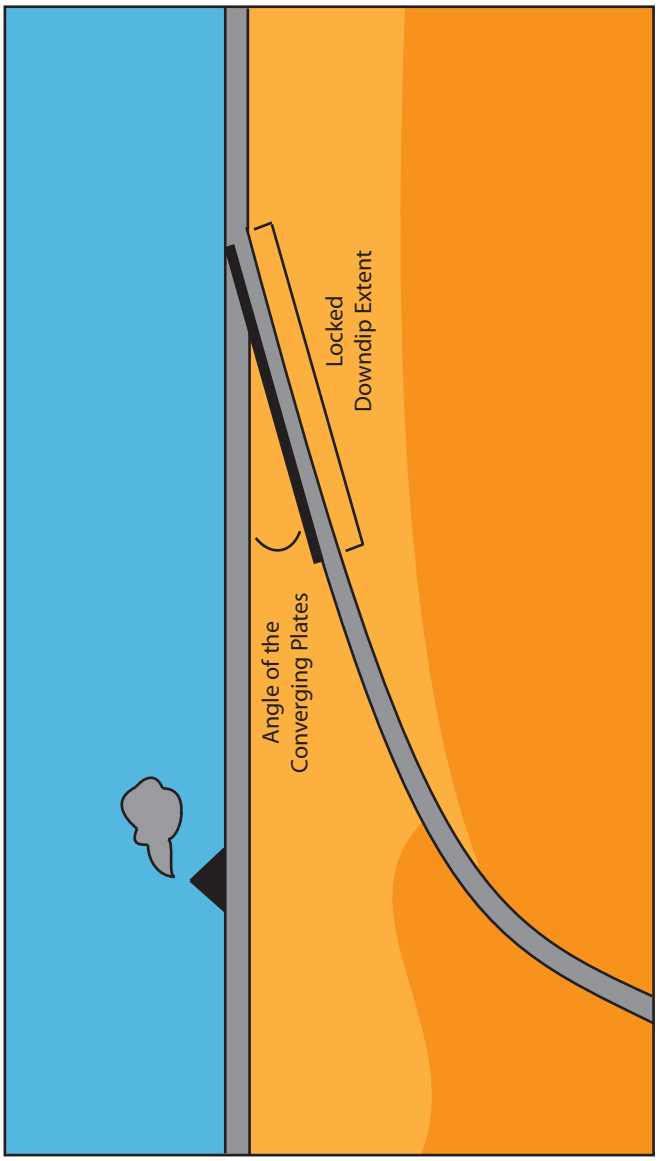

Figure 9. Schematic cross section showing two of the three variable parameters. Downdip extent refers to the length of the subducting slab which is locked with the overriding plate. The percentage of locking is modeled along this extent. Dip angle refers to the angle between the two coupled plates.

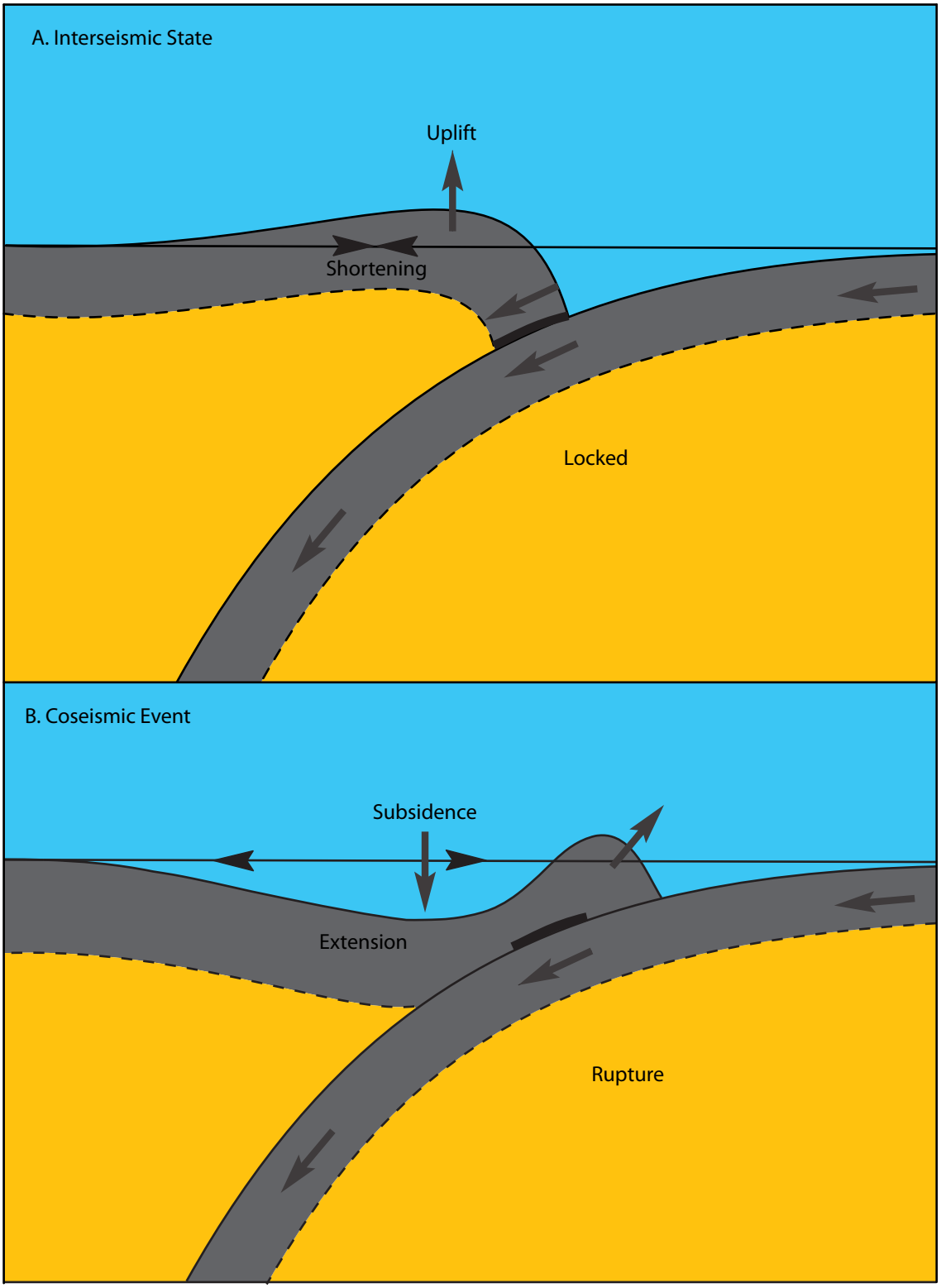

Figure 10. Schematic drawing of an earthquake cycle. (A) interseismic state in which the overlying plate deforms from the movement of the subducting plate against it. Deformation is characterized by uplift and shortening. (B) a coseismic event in which the locked portion of the subduction zone, indicated in a thick line, ruptures. This results in subsidence and extension arcward of the trench. Modified from Savage (1983).

in which strain is released, resulting in subsidence and extension of the overthrust lithosphere (Fig. 10, B; Savage, 1983). In the models, the downdip extent varied between 45 and 100 km in 15-25 km increments. The subduction angle varied between 10° and 40° in 5°-10° increments and percentage of locking varied between 25-100% in 25% increments.

The amount of predicted displacement differed depending on the parameter values in each model. The length of the locked downdip extent influenced the displacement by changing the area over which the slip was distributed. For example, a model with a 100 km downdip extent had less horizontal displacement over a larger surface area than a model with the same dip angle and a 45 km downdip extent (Fig. 11, A and B). Dip angle determined the depth that displacement was distributed through. For example, a model with a 30° dip had less horizontal displacement than a model with a 10° dip and the same downdip extent (Fig. 11, B and C). The amount of locking was directly proportional to the magnitude of predicted displacement. A model with 50% locking had half the displacement at each point along the transect than the same model with 100% locking (Fig 11, C and D).

Analyzing model fit with GPS data

The predicted displacement vectors from dislocation models were compared with observed residual displacements from GPS to find the set of parameters most consistent with the observed data. A 500 km long transect was drawn through Dominica perpendicular to the modeled subduction zone, extending from a central point on the modeled subduction zone trace towards the Caribbean plate interior. The predicted

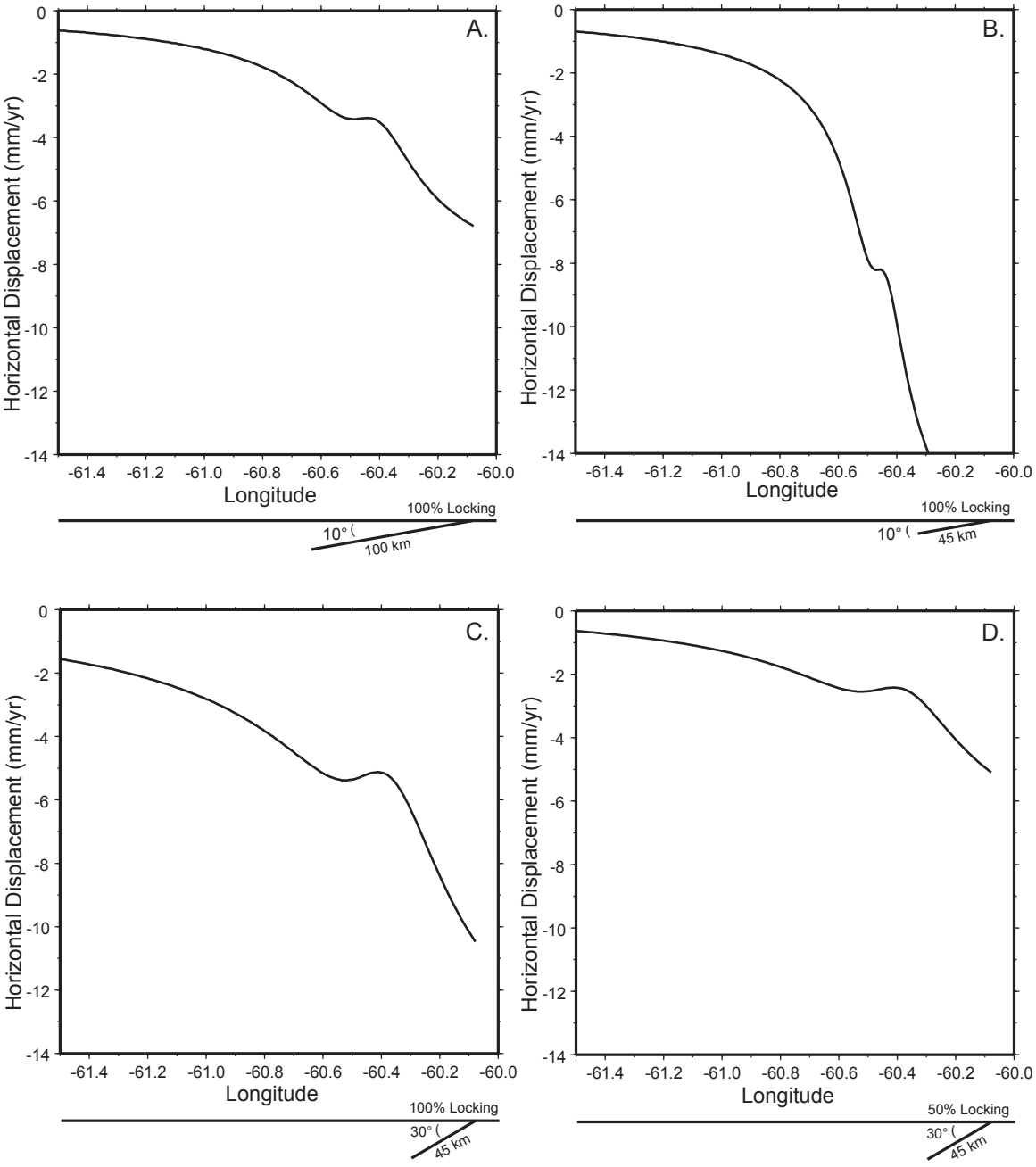

Figure 11. Horizontal displacement along the modeled transect for variable subduction zone geometries with 100% locking. (A) shows the westward surface displacement predicted for a subduction zone with a 10° dip angle and a 100 km locked downdip extent at 100% locking. (B) shows predicted westward displacement from a subduction zone with a 10° dip angle and a 45 km locked downdip extent at 100% locking. (C) shows predicted westward displacement from a subduction zone with a 30° angle and 45 km locked downdip extent at 100% locking. (D) shows predicted westward displacement from a subduction zone with a 30° angle and 45 km locked downdip extent at 50% locking.

horizontal and vertical displacement vectors were calculated from DISL in millimeters per year and compared to measured GPS vectors, an example of which is shown in Fig 12.

In order to better constrain the geometry and strain accumulation, GPS displacements from sites in Guadeloupe and Aves Islands were used in addition to campaign data from Dominica. The 28 GPS velocities (23 from Dominica, 4 from Guadeloupe, and 1 from Aves) were projected onto the same transect by translating the site distances from the subduction trench to the distance along the transect. The sites in Guadeloupe, just to the north of Dominica, create a transect oblique to the trench providing us with observed vectors at different distances from the source of deformation. Aves is attached to the rigid center of the Caribbean plate and far enough from the trench that there should be little or no surface displacement from locking along the subduction zone. This provides a data point farther along the transect to compare with the modeled displacements at such distances. The models are mostly constrained by the GPS sites in Guadeloupe and Aves rather than Dominica. Given the clustering of sites from Dominica within 30 km on the transect, most of the observations are redundant and of little effective utility in constraining the geometry of the system.

Statistical Analysis

To calculate the best-fit model, observed and modeled displacements were compared for each individual model. The difference between displacements for the vertical, longitudinal, and latitudinal components for each site provided the residuals (R):

(1) $\mathrm{Disp_{Obs}} - \mathrm{Disp_{Mod}} = R$,

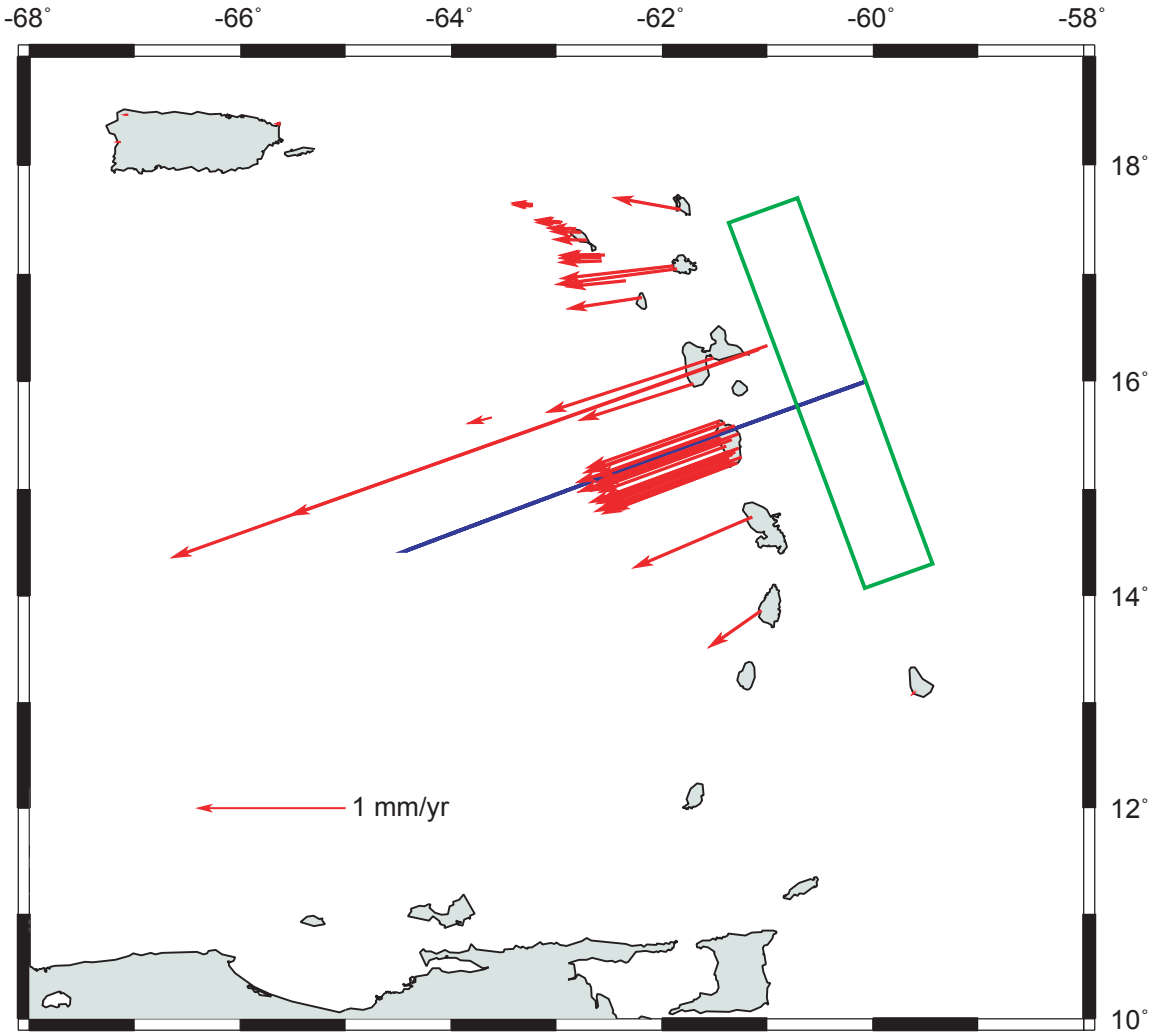

Figure 12. Predicted horizontal velocity vectors for the best-fit subduction model. The green rectangle traces the modeled subduction zone with locked interface, the transect of predicted motion is in blue, and the predicted displacement vectors are in red. Vectors are in a Caribbean-fixed reference frame for direction comparison with GPS residual vectors (see Fig. 6 and 7)

where $Disp_{Obs}$ is observed displacement and $Disp_{Mod}$ is modeled displacement. The number of degrees of freedom (df) for each model were calculated:

(2) $n_s\,(n_c) - n_p = df$,

where n_s are the number of site locations, n_c are the number of directional components, and n_p are the number of variable model parameters. From equations (1) and (2) the χ^2_R for each model was calculated:

(3) $$\frac{\sum \frac{R^2}{\sigma^2}}{df} = \chi^2_R$$

where σ is the error associated with each observed displacement.

The model with the lowest χ^2_R value fits the observed data best. This χ^2_R value also represents the error associated with the predicted displacements for the model. To determine the displacement on Dominica, a point in the center of the island at a distance of 150 km from the modeled subduction zone was used. The surface displacement predicted by the best-fit model at this distance from the trench is proportional to the effect of the predicted strain accumulation.

MODEL RESULTS

Based on the best-fit statistical comparisons between observed and predicted displacements, the GPS data constrain Lesser Antilles subduction geometry to a 75 km locked downdip slab length at a 10° dip angle with 50% locking. The predicted effect of strain accumulation from this geometry is 0.92±1.34 mm/yr to the west, 0.34±1.34 mm/yr to the south, and 0.01±1.34 mm/yr vertical in the center of Dominica. The predicted horizontal surface displacement is .95 mm/yr at 252°. This best-fit model has a χ^2_R of

1.34, the smallest value of all tested models, and both horizontal and vertical displacements are best-fit by this model (Fig. 13).

These surface displacement values suggest that the central Lesser Antilles are in a partially decoupled interseismic state because the predicted locking along the plates is neither fully coupled nor smoothly subducting. The model also suggests that plate motion is taken up by the elastic margins of the Caribbean plate because there is a vector of surface displacement related to the subducting lithospheres.

DISCUSSION

Model and GPS Comparisons

This study of GPS and modeled surface displacement helps constrain the subduction geometry and the magnitude of strain accumulation for the central Lesser Antilles. The best-fit model predicts slight positive vertical displacements, which agree with the observed positive vertical GPS vectors (Fig. 7). However, the horizontal displacements of the best-fit model and observed GPS data do not agree. Therefore the observed data do not define the subduction zone geometry and strain accumulation particularly well. By examining the observed data, one can see that vectors do not agree with purely tectonic deformation from coupling along the plate interface. Discrepancies between observed and modeled vectors may be attributed to the large uncertainties associated with the residual motion at many of the Dominica sites, poor site location, and the simplified nature of the model.

The Caribbean plate moves as a rigid system in the center yet deforms elastically along the margins. The data used to constrain the rigid motion of the plate is

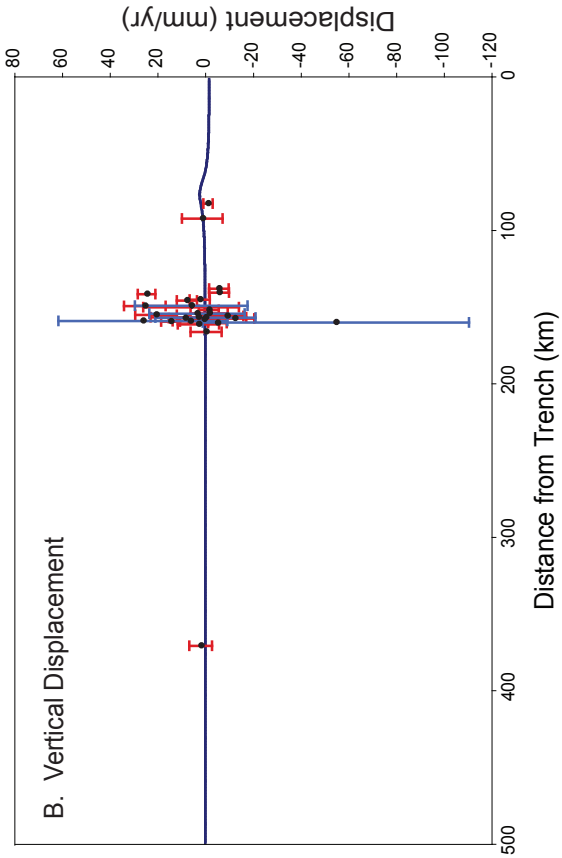

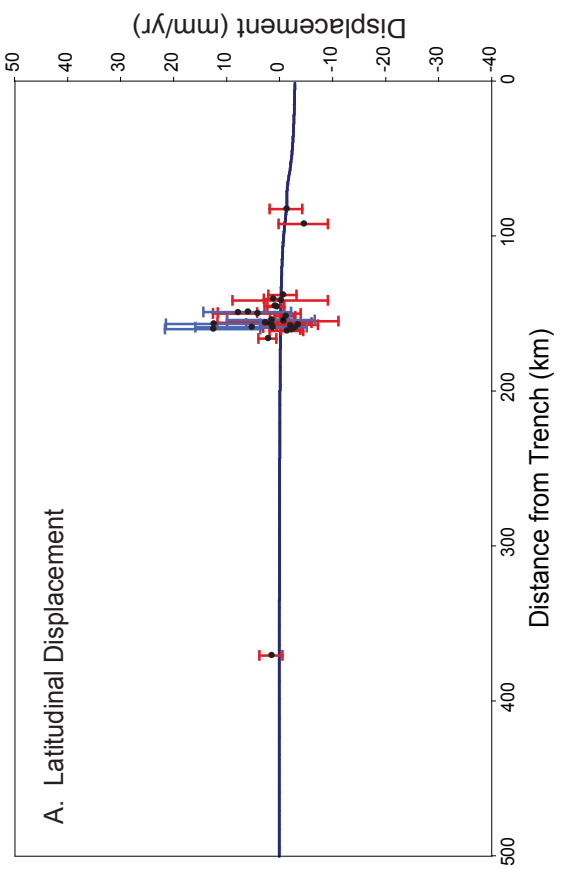

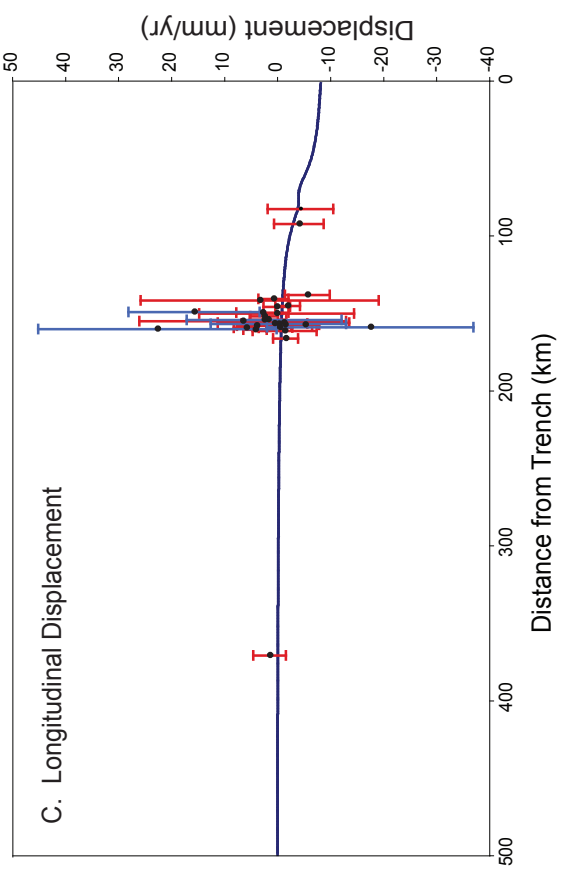

Figure 13. Graphs show observed GPS data plotted with the best-fit predicted velocities of our 2-D vertical transect. (A) latitudinal motion, (B) longitudinal motion, and (C) vertical motion. The dark blue line represents the modeled displacement along the 500 kilometer transect. Distances for GPS sites are projected onto the transect and are illustrated as black dots. Red error bars indicate velocity errors for sites with more than two years of data collection, whereas light blue error bars indicate velocity errors for sites with only two annual epochs of data.

predominantly taken from sites along the edges, creating a source of motion that is unrelated to overall Caribbean plate kinematics. This corruption of the data is most likely small, yet present. If residual motions are <1-2 mm/yr, however, they may still be used to constrain the secular motion of the Caribbean plate.

Furthermore, Dominica is an active volcanic island. Volcanism affects surface movement by magma chamber inflation and deflation, causing potentially large vertical and horizontal motions that are not related to subduction zone tectonics (Mattioli et al., 1998). Shallow seismic swarms from magma chamber movement occur in north and south parts of Dominica (SRU, 2000, Lindsay et al., 2003). There are few GPS sites on the island isolated from active volcanic centers. In addition, regional tectonism, such as movement along faults located on the Caribbean plate or the subduction of allochthonous ridges on the American plates (Bouysse and Westercamp, 1990) (Fig. 3), is another potential source for surface displacement not directly addressed by the simple locking models presented here.

Subduction zone geometry

The DISL model used to predict surface displacement was overly simplified when compared to the known geometry of the Lesser Antilles subduction zone. First, the trace of the subduction zone from gravity data, which shows an arc shaped trench (Fig. 2), is not a straight line as was modeled (Fig. 12). Second, I only modeled the northern half of the subduction zone at an average strike rather than the length of the subduction zone to make the model slightly more accurate. Third, the dislocation model only takes the first 75 km of the locked downdipping slab into account and assumes that movements in the

asthenosphere past the coupled Benioff zone would not influence deformation of the overlying Caribbean plate. Lastly, models had only a few values for each parameter over a wide range. A more thorough examination of a larger set of models would better constrain the Lesser Antilles subduction geometry and strain accumulation.

In constructing a cross-section from the model, the subducting slab was first extended below the Dominica with a constant 10° dip angle. This places the subducting slab ~13 km below the island arc. Earthquake hypocenter data shows this simplification is incorrect but confirms that the slab angle near the trench is at a very low angle (Feuillet et al., 2002). Dip increases with distance from the trench (Fig. 14). The model does not take slab curvature into account and assumes that only the first 75 km contribute to strain accumulation. This assumption is based on earthquake hypocenter data, which shows that the majority of earthquakes occur on the shallowly dipping Benioff zone. Future models should consider extending the slab after the modeled section with increasing dip to construct a more realistic cross-section (Fig. 15), rather than to keep it constant at a 10° angle.

Comparisons with Previous Studies

Despite notable differences in the best-fit model displacements and the observed data, our subduction zone geometry and strain accumulation findings are reasonable when compared with other data sets. In a transect between Dominica and Guadeloupe islands, earthquake hypocenters trace a 10° dip angle in the first ~75 km of the downgoing slab (Fig. 14). There is a sharp increase in dip angle with large cluster of interplate hypocenters are plotted just before this increase in dip angle in the Benioff zone

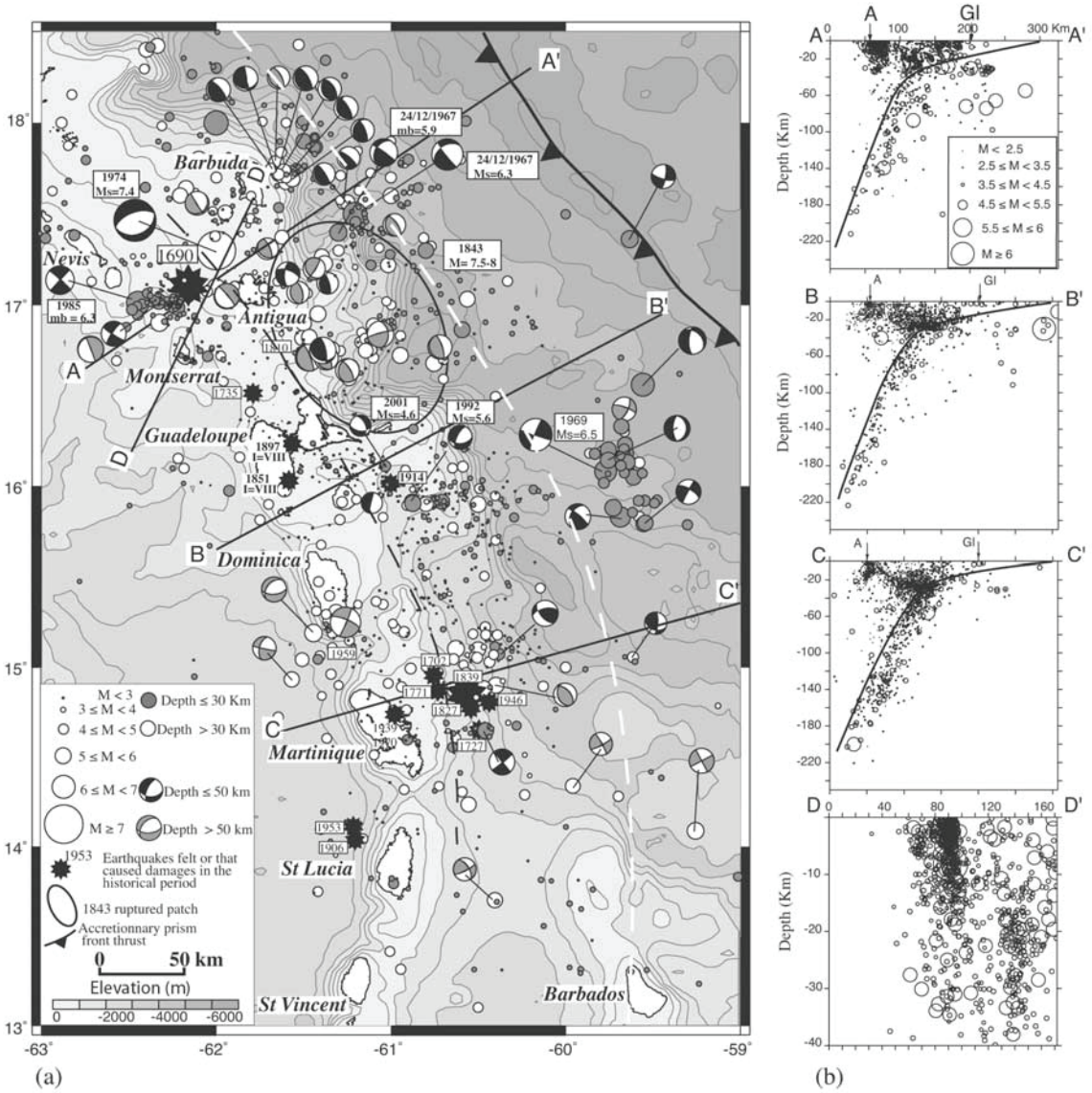

Figure 14. (a) Historical seismic data and focal mechanisms for the Lesser Antilles from Feuillet et al. (2002). The dotted black line represents the Benioff zone and the white dotted line represents the negative gravity anomaly. (b) Hypocenter depths are plotted with a black line representing the approximate subducting lithosphere location. Seismic data was attained from International Seismological Centre (ISC), Thatcham, United Kingdom; National Earthquake Information Service (NEIS), National Earthquake Information Center, U.S. Geological Survey; and Harvard University. Transects B-B' and C-C' trace a ~10° Benioff zone dip, increasing westwards to ~50-60° beneath the island arc.

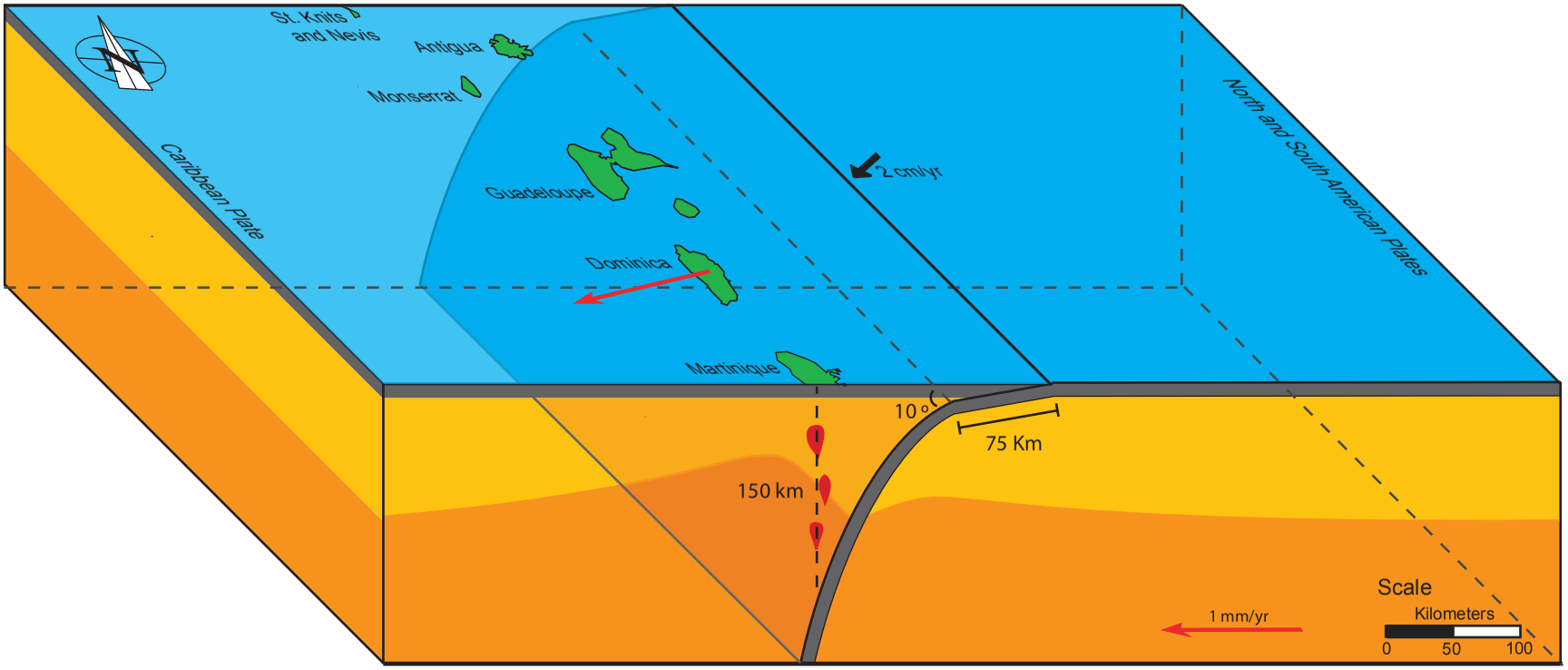

Figure 15. Cross section of the best-fit model for the data observed from Guadeloupe, Dominica, and Aves islands as of 2007. Model predicts an interseismic state of the subduction zone with 50% locking along a 75 km interface at a 10° angle. Predicted displacement for the center of Dominica is shown as red vector. Slab angle increases farther downdip, reaching approximately 50-60° in the arc region (Bouysse and Westercamp, 1990). This is also supported by hypocenters in the region reported by Feuillet et al. (2002). Schematic lithosphere, upper mantle and lower mantle boundaries are included with the dewatering of the downgoing slab pictured below the volcanic arc.

(Feuillet et al., 2002). The interpreted Benioff zone is located just trenchward of the island arc, as indicated above in the model and strain accumulation regime. The dip angle change occurs 75 km downdip from the strong negative gravimetric anomaly (Bowin, 1976) (Fig. 16), which is interpreted as the subduction zone trench (Bouysse and Westercamp, 1990). Not only does hypocenter data confirm the dip angle of the first 75 km of the downdip extent, but also that the plates are coupled along this portion of the interplate extent since the large majority of the interplate earthquakes take place along this extent. Furthermore, the drastic increase in dip angle also allows for hypocenters to reach ~150 km below the arc.

Seismic data suggest the Lesser Antilles have low seismicity and the subduction zone is partially decoupled (Stein et al., 1983) because there are relatively few earthquakes in the area. The occurrence of interplate earthquakes suggests that there must be some coupling between the converging plates. In a partially coupled system, strain accumulates for long periods of time before release in a seismic event. This is observed in historical seismic data for the Lesser Antilles (Dorel, 1981). If the subduction zone were entirely coupled, all movement of the converging plates would be taken up by the deformation of the margins, whereas if it were entirely decoupled, there would be no seismicity and thus no deformation.

In an elastic half-space model, deformation is most strongly felt near the subduction zone trace. Strain accumulates until the inboard edge of the Benioff zone and recovers linearly with distance from the subduction trace. Since Dominica is inboard of the Benioff zone in the model, there is only a small amount of predicted deformation. The slow convergence rate also impacts the amount of strain accumulation. Since strain

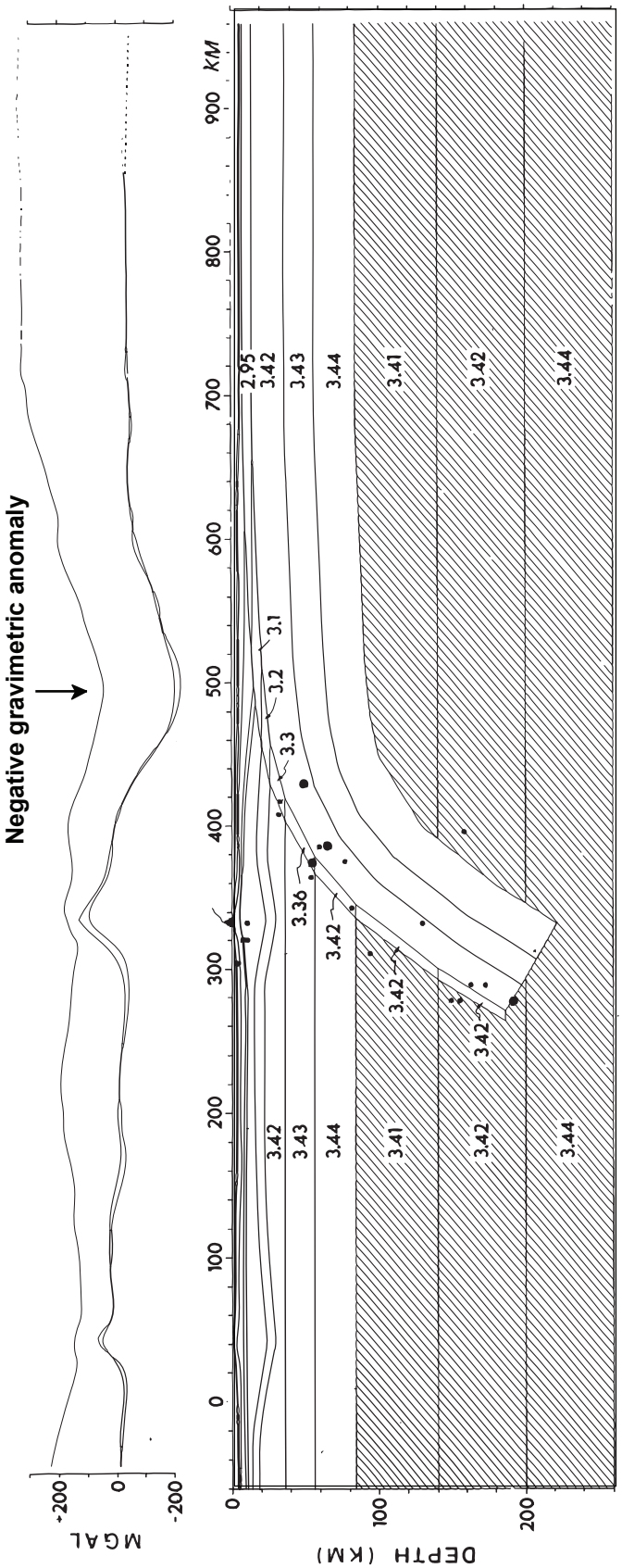

Figure 16. Model of crustal structure across Lesser Antillean island arc along lat 14°14′N. No vertical exaggeration. Density gradient in the mantle of lithosphere is simulated by three layers with increasing density with depth. Low-density zone (asthenosphere) indicated by inclined ruling. Above model upper profile is the complete Bouguer gravity anomaly, calculated assuming two-dimensionality of the bathymetry; lower solid line in the free-air gravity anomaly. Volcano symbol indicates the location of active volcanism on the island arc. Figure modified from Bowin (1976).

accumulation is measured in mm/yr surface displacements, a slower convergence rate results in slower displacements per year and therefore smaller associated strain.

The earthquake hypocenters plotted past this dip angle occur somewhat uniformly along the remainder of the downgoing slab. Seismic data from the larger events at depth suggest that earthquakes below ~100 km occur from intraplate extension in the slab rather than interplate coupling (Stein et al., 1983). The occurrence of intraplate slab extension agrees with suggestions that the old lithosphere sinks freely under its own weight (Isacks and Molnar, 1969). Intraplate earthquakes at this depth would therefore not have much affect on the strain accumulation and seismic hazard, and so modeling the subduction zone past the Benioff zone is unnecessary.

CONCLUSIONS

Models of subduction zone geometry using GPS data suggest that the central Lesser Antillean islands are in a state of interseismic deformation. The modeled strain accumulation and deformation agree with previous suggestions of an aseismic, partially decoupled system. The best-fit model of a 75 km downdip extent at 10° dip angle with 50% locking that produces such strain accumulation agrees well with published earthquake hypocenter data (Feuillet et al., 2002, Matson, 2006). Historical seismic data for this region shows that interseismic periods are punctuated by large rupture events along the plate interface. If the best-fit model is correct, it suggests that the central Lesser Antilles are accumulating strain that will be released in a large earthquake in the future.

Further studies of strain accumulation and comparisons to historical data may help estimate future seismic events. Future GPS data collection on Dominica and elsewhere in the central Lesser Antilles may help reduce errors in horizontal and vertical displacement vectors. A larger scale study including GPS site locations from the other Lesser Antillean islands alongside more precise modeling will better constrain the subduction zone geometry for the eastern Caribbean plate and strain accumulation in the Lesser Antilles.

ACKNOWLEDGEMENTS

First and foremost, I would like to thank the NSF-REU program for funding (award number EAR-0552765) and the University of Arkansas in Fayetteville for providing this research opportunity, GPS equipment and lab facilities. Furthermore, I would like to acknowledge my program and field advisor, Glen Mattioli, and program supervisors Steven James and Richard Styron. A special thanks goes to Henry Turner III for holding my hand through computer programming.

I would like to extend my thanks to Sarah Titus, my advisor at Carleton College, for reading and editing way too many drafts of this paper, and the Carleton College Geology Department along with the geology majors of 2008 for support and good times.

REFERENCES

Bouysse, P., and Westercamp, D., 1990, Subduction of Atlantic Aseismic Ridges and Late Cenozoic Evolution of the Lesser Antilles Island Arc: Tectonophysics, v. 175 p. 349-380.

Bowin, C., 1976, Caribbean gravity field and plate tectonics: Geological Society of America - Special Paper, v. 169, p. 79.

Carr, B. B., Mattioli, G.S., Jansma, P., Turner, H., Styron, R., Burch, M.J., Mansfield, C., Graham, S.E., and K. Fitzgerald, 2006, Ongoing Surface Deformation Studies of Dominica, BWI: GPS Results and Interpretations From the 2006 NSF-REU Campaign: Eos Trans. AGU, v. 87, no. 52, p. Fall Meet. Suppl., G53A-0867.

Davidson, R., H.L. Turner, B. Blessing, Parra, J., K. Fitzgibbon, P. Jansma, and G.S. Mattioli, 2004, 2003-2004 campaign GPS geodetic monitoring of surface deformation proximal to volcanic centers, Commonwealth of Dominica, Lesser Antilles: Eos Trans. AGU, v. 85, no. 47, p. Fall Meet. Suppl., G51A-0067.

DeMets, C., Mattioli, G.S., Jansma, P., Rogers, R., Tenorios, C., Turner, H.L. , 2007, Present motion and deformation of the Caribbean plate: constraints from new GPS geodetic measurements from Honduras and Nicaragua: Geological Society of America Special Paper, v. 428, p. 21-36.

DeMets, C., P. E. Jansma, G. S. Mattioli, T. H. Dixon, F. Farina, R. Bilham, E. Calais, P. Mann, 2000, GPS geodetic constraints on Caribbean-North American plate motion: Implications for plate rigidity and oblique plate boundary convergence: Geophysical Research Letters, v. 27, p. 437-440.

Dixon, T. H., 1991, An introduction to the Global Positioning System and some geological applications: Reviews of Geophysics, v. 29, no. 2, p. 249-276.

Dorel, 1981, Seismicity and seismic gap in the Lesser Antilles Arc and earthquake hazard in Guadeloupe: The Geophysical journal of the Royal Astronomical Society, v. 67, no. 3, p. 679-695.

Fauria, K., Styron, R.H., James, S., Turner, H.L., Ashlock, A., Cavness, C.L., Collier, X., Feinstein, R., Staisch, L., Williams, B., Mattioli, G.S., Jansma, P.E., Cothren, J., 2007, A Revised Caribbean Plate Motion Model: GPS Geodetic Results From the Dominica NSF- REU Site: Eos Trans. AGU, v. 88, no. 52, p. Fall Meet. Suppl., G21C-0657.

Feuillet, N., Manighetti, I., Tapponnier, P., Jacques E., 2002, Arc parallel extension and localization of volcanic complexes in Guadeloupe, Lesser Antilles: Journal of Geophyisical Research, v. 107, no. B12, p. 2331.

Graham, S., Turner, H.L., Mattioli, G.S., Jansma, P.E., Styron, R.H., Burch, M.J., Carr, B.B., FitzGerald, K., and C. Mansfield, 2007, GPS geodetic constraints on the November 21, 2004 Mw 6.3 earthquake off the northwest coast of Dominica: implications for in situ volatile solubilities and eruptions dynamics: Eos Trans. AGU, v. 88, no. 23, p. Jt. Assem. Suppl., G43B-12.

Heflin, M. B., Willy; Blewitt, Geoffrey; Freedman, Adam Paul; Hurst, Ken; Lichten, Steve; Lindqwister, Ulf J; Vigue, Yvonne; Webb, Frank; Yunck, Thomas P;

Zumberge, James, 1992, Global geodesy using GPS without fiducial sites: Geophysical Research Letters, v. 19, no. 2, p. 131-134.

Isacks, B., Molnar, P., 1969, Mantle earthquake mechanisms and the sinking of the lithosphere: Nature, v. 223, no. 5211, p. 1121-1124.

Jansma, P. E., and Mattioli, G. S., 2005, GPS results from Puerto Rico and the Virgin Islands: Constraints on tectonic setting and rates of active faulting: Geological Society of America, v. Special Paper 385, no. Active tectonics and seismic hazards of Puerto Rico, the Virgin Islands, and offshore areas, p. 13-30.

Larsen, S. C., 1992, Displacement modeling of dislocations, Ph.D. Thesis, California Institute of Technology, Pasadena.

Lindsay, J. M., Stasiuk M.V., Shepherd J.B., 2003, Geological history and potential hazards of the late-Pleistocene to Recent Plat Pays volcanic complex, Dominica, Lesser Antilles: Bulletin of Volcanology, v. 65, no. 2-3, p. 201-220.

Lindsay, J. M., Trumbell, R.B., Siebel, W., 2005, Geochemistry and petrogenesis of late Pleistocene to Recent volcanism in Southern Dominica, Lesser Antilles: Journal of Volcanology and Geothermal Research, v. 148, p. 253-294.

Macdonald, R., Hawkesworth, C.J., Heath, E., 2000, The Lesser Antilles volcanic chain: a study in arc magmatism: Earth Science Reviews, v. 49, p. 1-76.

Mao, A., Harrison, G.A., Dixon, T., 1999, Noise in GPS coordinate time series: Journal of Geophyisical Research, v. 104, no. B2, p. 2797-2816.

Mann, P., Schubert, C., Burke, K., 1990, Review of Caribbean Neotectonics, *in* Dengo, G., Case, J.E., ed., The Geology of North America: Boulder, CO, Geologic Society of America, p. 307-338.

Matson, S. E., 2006, Arc kinematics of the northern Lesser Antilles from GPS geodesy: M.S. Thesis, Geosciences, University of Arkansas, 77 p.

Mattioli, G. S., Dixon, T. H., Farina, F., Howell, E., Jansma P., Smith, A.L., 1998, GPS measurement of surface deformation around Soufriere Hills volcano, Montserrat from October 1995 to July 1996: Geophysical Research Letters, v. 25, p. 3417-3420.

National Earthquake Information Center (NEIC), 2007, Magnitude 7.4 - Martinique Region, Windward Islands, *in* United States Geological Survey, ed., USGS Earthquake Hazards Program.

Savage, J. C., 1983, A Dislocation Model of Strain Accumulation and Release at a Subduction Zone: Journal of Geophysical Research, v. 88, p. 4984-4996.

Sigurdsson, H., 1972, Partly welded pyroclast flow deposits in Dominica, Lesser Antilles: Transactions, v. 6, p. 307-312.

Seismic Research Unit (SRU), 2000, Volcano Hazard Report for Southern Dominica: Interpretation of 1998-2000 Earthquakes and Hazard Mapping Results: The University of the West Indies.

Speed, R. C., 1981, Geology of Barbados; implications for an accretonary origin: Oceanologica Acta, v. 4, p. 259-265.

Stein, S., Engeln, J.F., Wiens, D.A., 1982, Subduction seismicity and tectonics in the Lesser Antilles arc: Journal of Geophyisical Research, v. 87, no. B10, p. 8642-8664.

Stein, S., Engeln, J.F., Wiens, D.A., Speed, R.C., Fujita, K., 1983, Slow subduction of old lithosphere in the Lesser Antilles: Tectonophysics, v. 99, p. 139-148.

Sykes, L. R., Ewing, M., 1965, Seismitity of Caribbean Region: Journal of Geophyisical Research, v. 70, no. 20, p. 5065-&.

Tomblin, J. F., 1975, Reconnaissance report of Antigua, West-Indies, earthquake of October 8, 1974: Bulletin of the Seismological Society of America, v. 65, no. 6, p. 1553-1573.

Wadge, G., Shepherd, J.B., 1984, Segmentation of the Lesser Antilles subduction zone: Earth and Planetary Science Letters, v. 71, p. 297-304.

Yamashina, K., 1976, Drag model and crustal deformation in the Japanese islands: Program Abstract Seismology Society of Japan, v. 1, no. 56.

Zumberge, J. F., Heflin, M.B., Jefferson, D.C., Watkins, M.M., Webb, F.H., 1997, Precise point positioning for the efficient and robust analysis of GPS data from large networks: journal of Geophyisical Research - Solid Earth, v. 102, no. B3, p. 5005-5017.

Table 1. GPS site velocities and errors with distance from trench

Site	Distance	Error	Obs Lon	Error	Obs Lat	Error	Obs Vert
AVES	370.38	3.10	1.40	2.20	1.53	4.80	1.85
ATRU	149.01	4.94	2.76	3.73	7.84	8.70	25.31
BELV	145.31	2.50	0.07	1.60	0.58	4.20	7.64
BOTG	158.56	19.49	-17.58	10.49	12.45	35.40	26.09
BRDX	154.61	5.11	6.46	3.95	-0.71	8.70	20.62
CABR	156.88	2.59	-1.48	1.92	-3.42	6.90	8.34
CASS	151.55	2.85	2.43	1.64	-1.14	4.10	-1.55
CNCD	140.23	2.43	0.68	1.68	1.22	4.10	-5.85
COHT	158.76	6.21	-0.47	4.02	1.32	7.40	6.16
CONN	153.82	14.61	2.42	8.27	6.00	20.00	3.38
ELOI	156.20	3.66	0.49	2.44	2.15	6.50	2.81
FRSH	149.73	2.20	0.06	1.80	4.19	3.90	5.88
GOMM	157.57	2.31	3.90	1.81	-1.97	4.20	0.41
GSAV	160.02	6.04	4.14	3.19	-2.22	8.60	-5.21
GUIG	159.73	22.47	22.57	8.99	12.53	55.80	-54.81
NEWF	144.77	2.35	-1.99	1.62	0.91	3.70	2.24
NVEN	148.72	12.38	15.66	8.88	1.52	23.60	5.79
SCTT	160.84	2.62	-1.42	1.68	-1.39	3.90	2.79
SOIE	141.18	3.46	3.28	2.29	-0.20	6.80	24.48
SPAG	158.97	4.70	5.82	4.64	-2.83	8.10	14.47
SPNG	155.53	4.22	-1.22	2.64	2.73	7.80	-9.18
TETE	156.99	6.20	-5.30	3.07	1.51	8.50	-12.47
WOTT	153.60	2.37	1.72	1.69	-0.57	4.10	-1.65
WQ95	156.46	12.77	-0.27	8.28	5.27	21.00	-0.15
ADE0	91.85	1.70	-4.12	1.20	-4.58	2.00	1.17
FFE0	137.70	4.10	-5.72	3.00	-0.65	6.50	-5.77
PDB0	82.16	5.50	-4.41	4.00	-1.31	8.80	-1.22
HOUE	165.75	1.30	-1.60	1.10	2.21	2.20	-0.40

Table 2. Model parameters and χ^2_R for statistical best fit

Model #	1	2	3	4	5	6	7	8	9	10	11
Dip Angle	20	20	20	10	30	30	20	20	10	15	40
Downdip	45	100	60	60	45	60	45	45	45	45	45
Slip	2	2	2	2	2	2	1	1.5	2	2	2
Locking %	100	100	100	100	100	100	100	100	100	100	100
χ^2_R	1.41	2.24	1.49	1.37	1.45	1.57	1.39	1.44	1.38	1.39	1.46

Model #	12	13	14	15	16	17	18	19	20	21	22
Dip Angle	15	40	10	15	20	30	40	10	15	30	40
Downdip	60	60	75	75	75	75	75	100	100	100	100
Slip	2	2	2	2	2	2	2	2	2	2	2
Locking %	100	100	100	100	100	100	100	100	100	100	100
χ^2_R	1.42	1.56	1.44	1.57	1.68	1.76	1.69	1.84	2.10	2.15	1.88

Model #	23	24	25	26	27	28	29	30	31	32	33
Dip Angle	20	20	20	10	30	30	20	20	10	15	40
Downdip	45	100	60	60	45	60	45	45	45	45	45
Slip	2	2	2	2	2	2	1	1.5	2	2	2
Locking %	75	75	75	75	75	75	75	75	75	75	75
χ^2_R	1.39	1.82	1.42	1.36	1.41	1.46	1.39	1.43	1.39	1.38	1.42

Model #	34	35	36	37	38	39	40	41	42	43	44
Dip Angle	15	40	10	15	20	30	40	10	15	30	40
Downdip	60	60	75	75	75	75	75	100	100	100	100
Slip	2	2	2	2	2	2	2	2	2	2	2
Locking %	75	75	75	75	75	75	75	75	75	75	75
χ^2_R	1.38	1.47	1.37	1.44	1.51	1.57	1.55	1.57	1.73	1.80	1.66

Table 2 continued. Model parameters and χ^2_R for statistical best fit

Model #	45	46	47	48	49	50	51	52	53	54	55
Dip Angle	20	20	20	10	30	30	20	20	10	15	40
Downdip	45	100	60	60	45	60	45	45	45	45	45
Slip	2	2	2	2	2	2	1	1.5	2	2	2
Locking %	50	50	50	50	50	50	50	50	50	50	50
χ^2_R	1.39	1.55	1.38	1.37	1.39	1.41	1.39	1.43	1.40	1.39	1.40

Model #	56	57	58	59	60	61	62	63	64	65	66
Dip Angle	15	40	10	15	20	30	40	10	15	30	40
Downdip	60	60	75	75	75	75	75	100	100	100	100
Slip	2	2	2	2	2	2	2	2	2	2	2
Locking %	50	50	50	50	50	50	50	50	50	50	50
χ^2_R	1.37	1.42	1.34	1.37	1.41	1.45	1.46	1.41	1.50	1.56	1.52

Model #	67	68	69	70	71	72	73	74	75	76	77
Dip Angle	20	20	20	10	30	30	20	20	10	15	40
Downdip	45	100	60	60	45	60	45	45	45	45	45
Slip	2	2	2	2	2	2	1	1.5	2	2	2
Locking %	25	25	25	25	25	25	25	25	25	25	25
χ^2_R	1.40	1.42	1.39	1.39	1.40	1.39	1.41	1.42	1.41	1.40	1.40

Model #	78	79	80	81	82	83	84	85	86	87	88
Dip Angle	15	40	10	15	20	30	40	10	15	30	40
Downdip	60	60	75	75	75	75	75	100	100	100	100
Slip	2	2	2	2	2	2	2	2	2	2	2
Locking %	25	25	25	25	25	25	25	25	25	25	25
χ^2_R	1.39	1.41	1.36	1.37	1.38	1.40	1.41	1.36	1.40	1.43	1.44